Type I interferon activation and endothelial dysfunction in caveolin-1 insufficiency-associated pulmonary arterial hypertension

Salina Gairhe[a], Keytam S. Awad[a], Edward J. Dougherty[a], Gabriela A. Ferreyra[a], Shuibang Wang[a], Zu-Xi Yu[b], Kazuyo Takeda[c], Cumhur Y. Demirkale[a], Parizad Torabi-Parizi[a], Eric D. Austin[d], Jason M. Elinoff[a,1,2], and Robert L. Danner[a,1]

[a]Critical Care Medicine Department, National Institutes of Health Clinical Center, Bethesda, MD 20892; [b]Pathology Core, National Heart, Lung, and Blood Institute, National Institutes of Health, Bethesda, MD 20814; [c]Microscopy and Imaging Core Facility, Center for Biologics Evaluation and Research, US Food and Drug Administration, Silver Spring, MD 20993; and [d]Department of Pediatrics, School of Medicine, Vanderbilt University, Nashville, TN 37232

Edited by Akinori Takaoka, Hokkaido University, Sapporo, Japan, and accepted by Editorial Board Member Tadatsugu Taniguchi February 2, 2021 (received for review June 10, 2020)

Interferonopathies, interferon (IFN)-α/β therapy, and caveolin-1 (CAV1) loss-of-function have all been associated with pulmonary arterial hypertension (PAH). Here, CAV1-silenced primary human pulmonary artery endothelial cells (PAECs) were proliferative and hypermigratory, with reduced cytoskeletal stress fibers. Signal transducers and activators of transcription (STAT) and phosphoinositide 3-kinase (PI3K)/protein kinase B (AKT) were both constitutively activated in these cells, resulting in a type I IFN-biased inflammatory signature. *Cav1*$^{-/-}$ mice that spontaneously develop pulmonary hypertension were found to have STAT1 and AKT activation in lung homogenates and increased circulating levels of CXCL10, a hallmark of IFN-mediated inflammation. PAH patients with CAV1 mutations also had elevated serum CXCL10 levels and their fibroblasts mirrored phenotypic and molecular features of CAV1-deficient PAECs. Moreover, immunofluorescence staining revealed endothelial CAV1 loss and STAT1 activation in the pulmonary arterioles of patients with idiopathic PAH, suggesting that this paradigm might not be limited to rare CAV1 frameshift mutations. While blocking JAK/STAT or AKT rescued aspects of CAV1 loss, only AKT inhibitors suppressed activation of both signaling pathways simultaneously. Silencing endothelial nitric oxide synthase (NOS3) prevented STAT1 and AKT activation induced by CAV1 loss, implicating CAV1/NOS3 uncoupling and NOS3 dysregulation in the inflammatory phenotype. Exogenous IFN reduced CAV1 expression, activated STAT1 and AKT, and altered the cytoskeleton of PAECs, implicating these mechanisms in PAH associated with autoimmune and autoinflammatory diseases, as well as IFN therapy. CAV1 insufficiency elicits an IFN inflammatory response that results in a dysfunctional endothelial cell phenotype and targeting this pathway may reduce pathologic vascular remodeling in PAH.

interferon | inflammation | caveolin-1 | pulmonary artery endothelium | pulmonary arterial hypertension

Pulmonary arterial hypertension (PAH) is a progressive disease characterized by angio-obliterative vascular remodeling propagated, at least in part, by a dysfunctional pulmonary artery endothelium (1). While a growing armamentarium of pulmonary vasodilators have improved disease management, the occlusive arteriopathy of PAH has remained refractory to currently available therapies and is often fatal (2). Nonetheless, our understanding of PAH pathobiology, encompassing multiple cell types and aberrant signaling pathways, has advanced rapidly, raising hopes for a therapeutic breakthrough (3). Although universal approaches suitable for most patients would be highly desirable, the complexity of PAH and numerous conditions associated with its development have led to speculation that future treatment strategies may require targeting several dysregulated signaling pathways simultaneously and precision medicine therapeutics tailored to narrow patient subgroups.

A heterozygous frameshift mutation in caveolin-1 (*CAV1*) associated with decreased pulmonary artery endothelial CAV1 protein expression was recently identified as a rare cause of hereditary PAH (HPAH) (4). Pathologically remodeled pulmonary arterioles (5, 6) and plexiform lesions (7) in idiopathic PAH (IPAH) and other forms of PAH also exhibit decreased CAV1 expression, suggesting that CAV1 loss may be a generalizable condition not unique to *CAV1* mutation-associated PAH. However, the molecular pathogenesis of PAH due to CAV1 deficiency in human pulmonary artery endothelial cells (PAECs) is incompletely understood. CAV1 is a plasma membrane protein, located in 50- to 100-nm flask-shaped vesicles called caveolae, with myriad functions, including molecular scaffolding, trafficking, and signal transduction (8, 9). Within caveolae, CAV1 organizes signaling hubs by coupling with endothelial cell receptors and membrane-anchored signaling complexes, many of which are of known importance to PAH including bone morphogenetic protein receptor type 2 (BMPR2) (10), endothelial nitric oxide synthase (NOS3) (11), and intracellular kinase networks

Significance

Caveolin-1 (CAV1) loss-of-function mutations are a hereditary cause of pulmonary arterial hypertension (PAH), but wild-type CAV1 is also decreased in the vascular lesions of idiopathic and disease-associated PAH. Using human pulmonary artery endothelium, lung tissue, and serum from *Cav1*$^{-/-}$ mice, as well as fibroblasts and serum from patients with *CAV1* mutations, CAV1 deficiency produced a dysfunctional, PAH-like endothelial phenotype driven by an interferon-biased inflammatory response with constitutive STAT and AKT activation. Inhibiting JAK/STAT and PI3K/AKT reversed the aberrant endothelial phenotype of CAV1 loss and may similarly ameliorate pathologic vascular remodeling in PAH. Exogenous interferon alone reduced CAV1 expression and activated these same signaling pathways, suggesting that CAV1 insufficiency may contribute to the development of autoimmune and autoinflammatory disease-associated PAH.

Author contributions: S.G., J.M.E., and R.L.D. designed research; S.G., K.S.A., E.J.D., G.A.F., S.W., Z.-X.Y., K.T., and P.T.-P. performed research; E.D.A. contributed new reagents/analytic tools; S.G., K.S.A., E.J.D., S.W., C.Y.D., J.M.E., and R.L.D. analyzed data; and S.G., J.M.E., and R.L.D. wrote the paper.

Competing interest statement: The NIH Clinical Center Pulmonary Arterial Hypertension Program received support from Aadi Bioscience through a Cooperative Research and Development Agreement. The authors have no personal financial relationship with Aadi Bioscience or any other entity.

This article is a PNAS Direct Submission. A.T. is a guest editor invited by the Editorial Board.

[1]J.M.E. and R.L.D. contributed equally to this work.

[2]To whom correspondence may be addressed. Email: elinoffj@cc.nih.gov.

This article contains supporting information online at https://www.pnas.org/lookup/suppl/doi:10.1073/pnas.2010206118/-/DCSupplemental.

Published March 8, 2021.

(12, 13). Importantly, CAV1 amplifies BMPR2 signaling (14, 15) and genetic ablation of *Cav1* in mice leads to a general lack of caveolae, pulmonary hypertension, and cardiac abnormalities (16, 17). Furthermore, recent studies have revealed mechanisms by which CAV1 is depleted in the pulmonary endothelium, including tumor necrosis factor (TNF)-α– and nitric oxide-induced nitrosation of CAV1, eventually leading to its proteasome-dependent degradation (5), as well as release of CAV1 containing extracellular vesicles following endothelial injury in vitro and in vivo (6).

Less is known about the effects of CAV1 deficiency on inflammation and how they may influence the development or progression of PAH. Disrupted B cell receptor signaling in *Cav1* knockout ($Cav1^{-/-}$) mice has recently been linked to impaired central tolerance and autoimmunity (18). Similarly, CAV1 is suppressed in psoriatic plaques and CAV1 silencing activates JAK2/STAT3 (signal transducers and activators of transcription) in keratinocytes (19). Essential for full activation and propagation of JAK/STAT/interferon (IFN) responses (20, 21), phosphoinositide 3-kinase (PI3K)/protein kinase B (AKT) signaling is constitutively activated in CAV1-silenced endothelial cells (12) and the pulmonary arteries of $Cav1^{-/-}$ mice (13). Importantly, type I IFNs cause drug-induced PAH (22) and play a prominent role in autoimmune diseases associated with the development of PAH (23). In addition, two type I interferonopathies were recently linked to pulmonary hypertension and pulmonary vasculopathy: chronic atypical neutrophilic dermatosis with lipodystrophy and elevated temperature due to loss-of-function mutations in the *PSMB8* gene (24), and stimulator of IFN response cGAMP interactor 1 (STING)-associated vasculopathy with onset in infancy (SAVI) due to a gain-of-function mutation in *TMEM173* (25). Nonetheless, whether CAV1 loss triggers a self-sustaining inflammatory response in endothelial cells has not been explored. Here, using small-interfering RNA (siRNA) knockdown of *CAV1* in human PAECs and $Cav1^{-/-}$ mice, as well as serum and fibroblasts from patients with *CAV1* mutations, the consequences of CAV1 deficiency were investigated, focusing on endothelial cell phenotype, signaling, and inflammation.

Results

CAV1 Silencing in PAECs Induced a Proliferative, Apoptosis-Resistant, Invasive, and Inflammatory Phenotype with Cytoskeleton Remodeling. To determine the specific role of CAV1 loss in human PAEC pathobiology, CAV1 was knocked down using a targeted siRNA approach (siCAV1). CAV1 mRNA and protein were both significantly reduced in these cells (*SI Appendix*, Fig. S1*A*). Precapillary angioproliferative lesions, the pathological hallmark of PAH, are hypothesized to be driven by a hyperproliferative and apoptosis-resistant endothelium (1). Similarly, compared to control siRNA-transfected PAECs (siCTRLs), CAV1-silenced PAECs displayed aberrant proliferation (Fig. 1*A*), apoptosis resistance (Fig. 1*B*) in response to serum and growth factor withdrawal, and increased migration (Fig. 1*C*). Given that PAEC migration starts with the loss of membrane proteins involved in cell–cell contact (26), vascular endothelial cadherin (VE-cadherin) and platelet endothelial cell adhesion molecule (PECAM)1 were examined by immunofluorescence labeling and confocal imaging. In contrast to intense staining of VE-cadherin and PECAM1 at endothelial cell–cell junctions in control PAECs, staining was diminished in CAV1-silenced cells (Fig. 1 *D* and *E*). Furthermore, VE-cadherin and PECAM1 staining was no longer specifically localized to cell junctions in CAV1-deficient PAECs, but instead diffuse and, in part, cytoplasmic. Importantly, CAV1 silencing also led to cytoskeletal remodeling, as shown by a decrease in filamentous actin polymerization (F-actin, stress fibers) (Fig. 1*F*). Expression of ICAM1 and VCAM1, markers of endothelial activation, were also increased in CAV1-silenced PAECs (Fig. 1*G* and *SI Appendix*, Fig. S1*B*). Similarly, the secretion of interleukin (IL)-6 and IL-8, inflammatory cytokines, was increased two- to threefold in CAV1-silenced PAECs compared to siCTRLs (Fig. 1*H* and *SI Appendix*, Fig. S1*B*). Taken together, these results indicate that CAV1 loss leads to a highly dysfunctional endothelial cell phenotype characterized by proliferation, apoptosis resistance, hypermigration, and inflammatory activation.

Prominent IFN Gene Signature in CAV1-Deficient PAECs. Genome-wide expression profiling was performed to unbiasedly assess the impact of CAV1 deficiency on gene transcription. Selection of differentially expressed transcripts following CAV1 gene silencing (false-discovery rate [FDR] ≤ 10% and fold-change [FC] ≥ 1.2) yielded 344 unique genes (Dataset S1); 227 were up-regulated and 117 were down-regulated. Using Ingenuity Pathway Analysis (IPA), CAV1-silenced PAECs showed strong enrichment for antiviral response ($P = 1.05 \times 10^{-16}$), cell movement ($P = 2.01 \times 10^{-12}$), systemic autoimmunity ($P = 2.39 \times 10^{-12}$), and endothelial cell proliferation ($P = 3.11 \times 10^{-9}$) (Fig. 2*A*). IFN signaling was identified by IPA as the top canonical pathway ($P < 0.0001$) (*SI Appendix*, Fig. S2*A*) predicted to be activated in CAV1-silenced PAECs (z-score = 2.828). In addition to a prominent IFN gene signature, leukocyte adhesion and diapedesis, pattern recognition receptor signaling, innate and adaptive immune cell communication, and activation of IFN response factor (IRF) by cytosolic pattern recognition receptors were among the most highly enriched canonical pathways following CAV1 loss in PAECs ($P < 0.01$ for all) (*SI Appendix*, Fig. S2*A*). Although induction of IFN-like gene expression has been reported in cells exposed to siRNA, the short length, low concentration, and low GU-content of the CAV1-specific siRNA used here make an off-target, IFN response unlikely (27).

Gene-expression changes in CAV1-silenced PAECs were also analyzed by gene set enrichment analysis (GSEA). In contrast to bioinformatic analyses that rely on a subset of genes defined by selection filters (e.g., FDR thresholds or FC differences), GSEA is a computational method that rank orders the entire gene-expression dataset and determines whether a priori defined gene sets demonstrate significant differences between two biological phenotypes (siCAV1 vs. siCTRL). The five most significantly enriched gene sets in CAV1-silenced PAECs were IFN-α, IFN-γ, and inflammatory responses, as well as IL6/JAK/STAT3 and TNF-α–induced NF-κB signaling (FDR < 0.01 for all) (*SI Appendix*, Fig. S2*B*). Collectively, both IPA- and GSEA-based thematic analyses identified an IFN inflammatory signature as the most highly enriched transcriptomic response in CAV1-silenced PAECs.

Next, using ClueGO (v2.5.4) with gene ontology (GO; GO_ImmuneSystemProcesses) and Reactome pathway annotation terms, a functional network analysis of up-regulated transcripts in CAV1-silenced PAECs (FDR ≤ 10% and FC ≥ 1.2; $n = 227$) reinforced activation of IFN signaling as a prominent consequence of CAV1 loss in PAECs (Fig. 2*B*). To further analyze and substantiate the apparent association of CAV1 loss with an IFN inflammatory response in PAECs, differentially expressed transcripts were analyzed in Interferome v2.01, a database that enables reliable identification of IFN response genes based on collated experimental data from nearly 200 human datasets of cells, tissues, or subjects treated with IFNs. Notably, >80% (283 of 344) of the transcripts differentially expressed in CAV1-deficient PAECs were identified as IFN-regulated, mostly annotating to type I and II responses (*SI Appendix*, Fig. S2*C*).

The constitutive activation of an IFN gene signature in CAV1-silenced PAECs was validated by quantitative real-time PCR (qRT-PCR) in six different donors to determine donor-to-donor variability (*SI Appendix*, Table S1). There was good correlation between microarray and qRT-PCR determined FC ($r = 0.79$, $P = 0.004$) (*SI Appendix*, Figs. S2*D* and S3) for a subset of IFN response genes (*CCL5*, *CXCL5*, *CXCL11*, *IFIT1*, *IFIT3*, *IRF9*, *ISG15*, *EDN1*, *SPRY1*, *DCBLD2*, and *LAMP3*). Thus, CAV1 loss alone induced an IFN-biased, proinflammatory signature in PAECs.

Expression of a strong IFN response gene signature in our transcriptomic analysis indicated that endothelial cell dysfunction

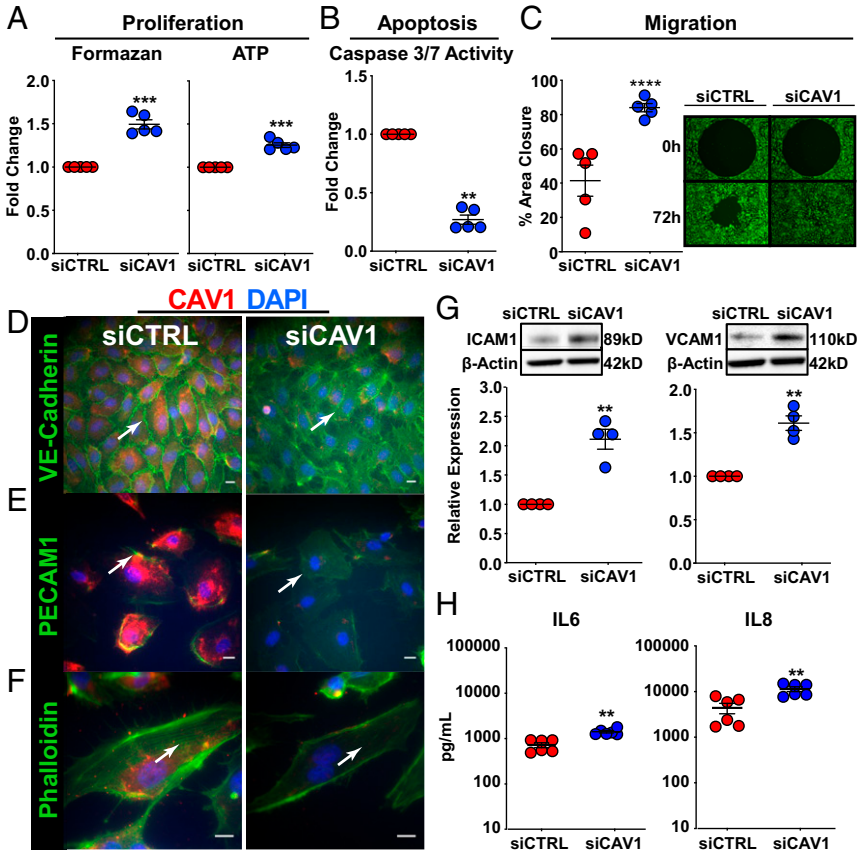

Fig. 1. *CAV1* gene silencing in primary human PAECs leads to a proliferative, apoptosis-resistant, and hypermigratory phenotype with remodeling of the cytoskeleton and inflammatory activation. (*A*) Cell proliferation, assessed by MTS and ATP assays, was significantly increased in CAV1-silenced PAECs compared to siCTRL. After CAV1 knockdown (48 h), PAECs were transferred to 96-well plates for 6 h, then serum-starved for 24 h, followed by complete media for 72 h to assess proliferation. Data presented as mean FC ± SE. (*B*) CAV1-deficient PAECs demonstrated significantly less apoptosis following serum and growth factor withdrawal compared to siCTRL-transfected cells. After CAV1 knockdown (48 h), PAECs were transferred to 96-well plates in serum and growth factor-free media. Caspase 3/7 activity, a marker of apoptosis, presented as mean ± SE. (*C*) Cell migration using the Oris ProCell migration assay was significantly increased in CAV1-silenced PAECs compared to siCTRL. After CAV1 knockdown (48 h), PAECs were transferred to 96-well plates containing a circular gel insert and allowed to adhere for 6 h. Cells were then serum-starved for 24 h, returned to complete media, and the insert was removed. Percent closure (mean ± SE) of the defect was assessed 72 h later. A representative image at 0 and 72 h is shown (*Right*; 10 × magnification). (*D*) VE-cadherin, (*E*) PECAM1/CD31, and (*F*) Phalloidin (F-actin) immunofluorescence staining (all green; white arrow), as well as CAV1 (red) and DAPI (nuclear counterstain; blue) in PAECs 48 h after CAV1-silencing or siCTRL. Results were similar in three independent experiments. (Scale bars, 20 μm.) (*G*) Immunoblotting of whole-cell lysates collected 48 h after siRNA knockdown demonstrated a significant increase in ICAM1 and VCAM1 expression in CAV1-deficient PAECs. Densitometric quantification of ICAM1 and VCAM1 protein normalized to β-actin and relative to siCTRL presented as mean ± SE. Representative Western blots shown in the *Insets*. (*H*) IL-6 and IL-8 in conditioned media from CAV1-silenced compared to siCTRL PAECs measured by ELISA at 48 h. Data presented as mean ± SE and replication throughout are independent experiments using different PAEC donors. $^{**}P < 0.01$, $^{***}P < 0.001$, $^{****}P < 0.0001$.

from CAV1 loss might be a direct consequence of a constitutive IFN inflammatory response. Therefore, we hypothesized that loss of CAV1 dysregulated IFN signal transduction pathways, potentially explaining the roles of both CAV1 and IFN in PAH pathobiology. This concept was then further tested in vitro and in vivo.

Activation of a Type I IFN Inflammatory Response in CAV1-Silenced Human PAECs. To identify molecules and pathways involved in the constitutively activated IFN response seen in CAV1-deficient PAECs, we first assessed the expression of type I (IFN-α, IFN-β) and type II (IFN-γ) IFNs. Secreted IFN-α and IFN-β protein were significantly increased in CAV1-silenced, human PAECs compared to nontargeting siRNA controls (Fig. 3*A*). As expected, IFN-γ was not detected in either control or CAV1-silenced PAECs. Next, IFN signaling through the JAK/STAT pathway was investigated. STAT1, STAT2, and STAT3 mRNA were all increased in CAV1-silenced PAECs compared to controls (*SI Appendix*, Fig. S4*A*). Similarly, both total and activated (phosphorylated) STAT1 and STAT3 proteins were increased, denoting canonical JAK/STAT activation (Fig. 3*B*).

STAT signaling interacts with and activates IRFs, including IRF3 and IRF7, thereby inducing the transcription of canonical type I IFN-response genes. IRF3 and IRF7 activation was further explored in PAEC nuclear lysates using DNA-binding ELISAs. CAV1 loss activated both IRF3 and IRF7 DNA binding to cognate IFN response elements (Fig. 3*C*), further confirming the activation of type I IFN responses. Furthermore, CXCL10, a prototypical IRF3- and IRF7-dependent chemokine, was robustly induced in CAV1-silenced PAECs (Fig. 3*D* and *SI Appendix*, Fig. S4*B*). IRF3 activation and the induction of a type I IFN response can occur downstream of STING1 and TANK binding kinase 1 (TBK1) phosphorylation and activation in response to intracellular DNA fragments (28). Notably, CAV1 silencing had no impact on either activated (pTBK1^{Ser172}) or total TBK1 (*SI Appendix*, Fig. S4*C*), suggesting that the constitutive type I IFN response associated with CAV1 loss was STING:TBK1-independent. Finally, luciferase reporter assays driven by either the IFN-stimulated response element

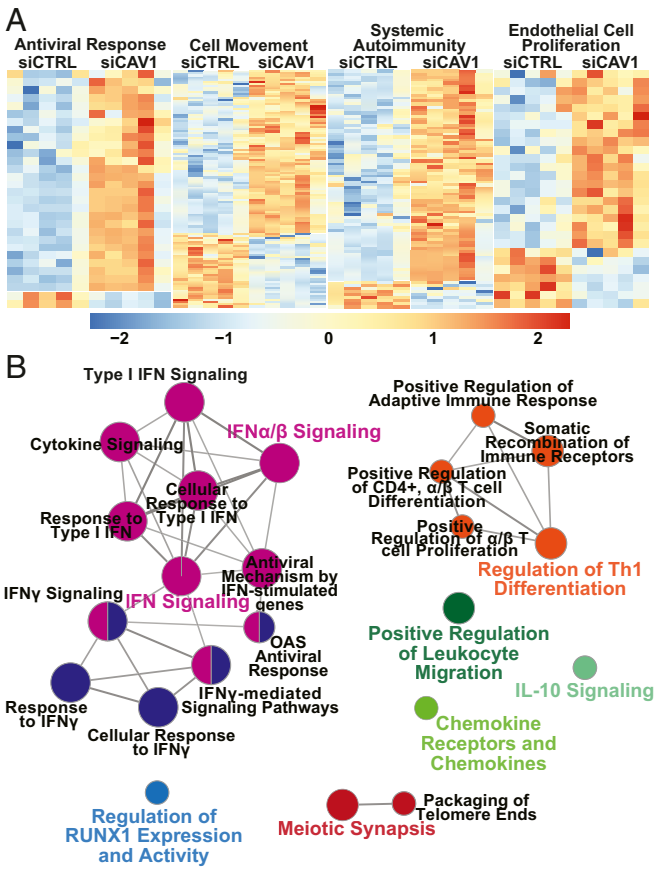

Fig. 2. Type I IFN response gene signature in CAV1-deficient primary human PAECs. (*A*) Differentially expressed genes within four top biofunctions are displayed as heat maps: antiviral response (n = 30 genes, $P = 1.05 \times 10^{-16}$); cell movement (n = 114 genes, $P = 2.01 \times 10^{-12}$); systemic autoimmunity (n = 79 genes, $P = 2.39 \times 10^{-12}$); and endothelial cell proliferation (n = 28 genes, $P = 3.11 \times 10^{-9}$). Orange signifies expression above and blue below the mean within each row. For full annotations, see Dataset S1. (*B*) Up-regulated transcripts in CAV1-silenced PAECs (FDR ≤ 10% and FC ≥ 1.2; n = 227) were used to create a functionally organized network of immune related pathways and functions in ClueGO (v2.5.4) based on GO (GO_ImmuneSystemProcesses) and Reactome pathway annotation terms. Node size corresponds to the enrichment significance of the terms and central nodes are denoted by colored text. Pathway threshold set at $P \leq 0.01$.

(ISRE) or γ-IFN activation site (GAS) tandem repeat-containing promoters demonstrated augmented responses to IFN-α/IFN-β, or IFN-γ stimulation, respectively, in CAV1-silenced human EAhy926 endothelial cells compared to siCTRLs (Fig. 3*E* and *SI Appendix*, Fig. S4*D*). Collectively, CAV1 loss was shown to constitutively activate endogenous type I JAK/STAT/IFN signaling by the following evidence: 1) increased IFN-α and IFN-β expression and secretion; 2) phosphorylation and activation of STAT1 and STAT3; 3) increased DNA binding of IRF3 and IRF7 to cognate promoter sequences; 4) the induction of IFN target genes including canonical CXCL10; and 5) activation of IFN reporter assays.

JAK/STAT and PI3K/AKT Activation in *Cav1*$^{-/-}$ Mice Recapitulate CAV1 Silencing in Human PAECs. In addition to JAK/STAT pathway activation, type I IFN signaling has been reported to activate MEK/ERK1/2, p38 and PI3K/AKT in some cell types and PI3K/AKT activation is essential to fully propagate JAK/STAT signaling and IFN responses (20, 21). Notably, MEK/ERK1/2 and PI3K/AKT signaling, oncogenic pathways associated with cell proliferation, have been shown to be constitutively activated in the heart and lungs of *Cav1*$^{-/-}$ mice (13, 29). Therefore, we next sought to explore these pathways in CAV1-silenced PAECs. While the MEK/ERK1/2 pathway was not affected, AKT activity as determined by phosphorylation at serine 473 (pAKT^{Ser473}) was increased in CAV1-silenced PAECs (*SI Appendix*, Fig. S5).

In order to investigate the in vivo relevance of JAK/STAT and PI3K/AKT activation and the resulting IFN inflammatory response observed in CAV1-silenced PAECs, whole-lung lysates from *Cav1*$^{-/-}$ mice were examined by Western blotting. As expected, CAV1 was detected in wild-type, but not *Cav1*$^{-/-}$ mice (*SI Appendix*, Fig. S6). Both total and activated (phosphorylated) STAT1 were elevated in CAV1-null mice compared to wild-type controls (Fig. 4*A*). Similarly, both total and pAKT^{Ser473} were also increased in whole-lung lysates from *Cav1*$^{-/-}$ mice (Fig. 4*B*). Consistent with these findings, circulating CXCL10 was elevated in *Cav1*$^{-/-}$ mice compared to controls (Fig. 4*C*). These in vivo results further corroborate STAT and AKT activation and the IFN inflammatory signature of CAV1-silenced human PAECs.

Proliferative, Hypermigratory Phenotype and STAT Activation in Dermal Fibroblasts from Patients with CAV1 Mutations and HPAH. Pulmonary vascular cell proliferation, migration, and inflammation are hallmarks of PAH and CAV1-silenced PAECs recapitulated these disease-defining aspects of PAH pathobiology. Next, fibroblasts from three HPAH patients with CAV1 loss-of-function mutations were investigated in order to determine whether these cells harbored similar phenotypic and signaling abnormalities. Compared to healthy control subjects, dermal fibroblasts from HPAH patients with a heterozygous frameshift mutation, resulting in a dominant-negative form of CAV1 (30), exhibited lower CAV1 protein expression (*SI Appendix*, Fig. S7*A*), increased proliferation (Fig. 5*A*), resistance to apoptosis (*SI Appendix*, Fig. S7*B*), and a hypermigratory phenotype (Fig. 5*B*). In addition, like CAV1-silenced PAECs, ICAM1 and VCAM1 (*SI Appendix*, Fig. S7*C*), as well as both total and activated STAT1 and STAT3, were all increased in fibroblasts from patients with CAV1 mutation-associated HPAH (Fig. 5*C*). These cells displayed high pAKT^{Ser473} levels relative to control fibroblasts (Fig. 5*C*), and secreted CXCL10 was also elevated in culture supernatants from HPAH-patient cells (Fig. 5*D*). Thus, dermal fibroblasts from HPAH patients with CAV1 mutations displayed an abnormal cellular and molecular phenotype that mirrored our findings in CAV1-silenced PAECs. Importantly and consistent with an underlying IFN inflammatory response in vivo, serum CXCL10 concentrations were significantly elevated in HPAH patients carrying CAV1 disease-associated mutations compared to noncarrier controls (Fig. 5*D*). Finally, in support of a broader role for CAV1-deficiency–associated IFN activation, immunofluorescent staining of explanted lung tissue from IPAH patients demonstrated reduced CAV1 expression along with activation (phosphorylation) of STAT1 in distal PAECs (Fig. 5*E*).

JAK/STAT Inhibitors Suppress the IFN Signature and the Proliferative and Migratory Phenotype of CAV1-Silenced PAECs. The JAK/STAT/IFN pathway was explored as a potential therapeutic target in PAH associated with CAV1 loss. Three currently available, Food and Drug Administration (FDA)-approved JAK inhibitors were tested: baricitanib, ruxolitinib, and tofacitinib. A clinically achievable concentration of all three JAK inhibitors (100 nM) (25) substantially blocked CAV1 loss-mediated STAT1 activation in human PAECs (*SI Appendix*, Fig. S8*A*). Ruxolitinib modestly reduced total STAT1 expression, whereas baricitanib and tofacitinib had no effect. Baricitanib, ruxolitinib, and tofacitanib abrogated elevated CXCL10 secretion in CAV1-silenced PAECs (Fig. 6*A*), and normalized CAV1-silenced PAEC proliferation (Fig. 6*B*, measured by BrdU incorporation, and *SI Appendix*, Fig. S8*B*, measured by formazan production) and migration (Fig. 6*C*). Yet, JAK/STAT inhibitors did not block AKT activation (*SI Appendix*, Fig. S8*C*), suggesting this approach may not fully rescue the cellular consequences of CAV1

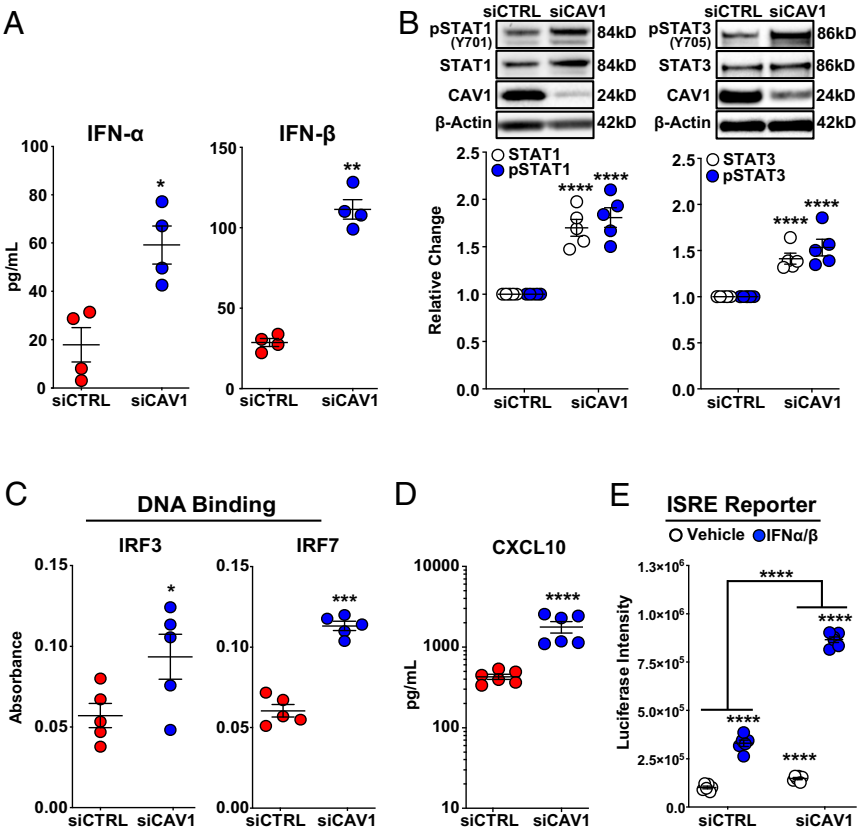

Fig. 3. Constitutive activation of IFN signaling due to CAV1 loss-of-function in primary human PAECs. (*A*) IFN-α and IFN-β, measured by ELISA, were significantly higher in conditioned media 48 h after CAV1-silencing compared to siCTRL-transfected PAECs. Data presented as mean ± SE. (*B*) Whole-cell lysate immunoblotting 48 h after CAV1 knockdown demonstrated a significant increase in both total and phosphorylated (activated) STAT1 and STAT3. Densitometric quantification of protein normalized to β-actin and relative to siCTRL presented as mean ± SE with representative Western blots. (*C*) Nuclear protein isolated from CAV1-silenced PAECs 48 h after knockdown demonstrated significantly increased IRF3 and IRF7 DNA binding compared to siCTRL-transfected cells (mean absorbance ± SE). (*D*) CAV1 loss in PAECs led to significant increase in CXCL10 protein. Cell supernatants collected 48 h after CAV1 knockdown. CXCL10 measured by ELISA presented as mean ± SE. (*E*) ISRE activity was significantly higher in CAV1-silenced human EAhy926 endothelial cells in the absence and presence of IFN-α/β stimulation. Additionally, CAV1-silenced EAhy926 cells displayed significantly greater response to IFN-α/β stimulation compared to siCTRL-transfected cells. Human EAhy926 endothelial cells were stably transfected with ISRE reporter constructs and then transiently transfected with CAV1-specific or nontargeting control siRNA. After siRNA transfection (48 h), cells were treated with IFN-α/β (10 U/mL) or vehicle alone (PBS with 0.1% BSA) for 5 h. Luciferase intensity presented as the mean ± SE. Each independent experiment used different PAEC donors. $*P < 0.05$, $**P < 0.01$, $***P < 0.001$, $****P < 0.0001$.

loss. Notably, JAK/STAT inhibitors have ameliorated pulmonary hypertension in some patients with myelofibrosis (31), while others have experienced disease worsening (32).

PI3K-AKT Signaling Axis in the CAV1 Loss-Mediated Proliferative Phenotype of PAECs. To investigate the role of PI3K/AKT activation as a driver of phenotypic abnormalities and type I IFN responses associated with CAV1 loss, PI3K/AKT signaling was blocked with LY294002 (15 μM) and Wortmannin (50 nM), two pan-PI3K inhibitors. These concentrations of LY294002 and Wortmannin were previously shown to inhibit PI3K signaling in endothelial cells (33). As expected, PI3K inhibition significantly reduced AKT activation. Furthermore, these inhibitors also prevented STAT1 activation in CAV1-silenced PAECs (Fig. 7*A* and *SI Appendix*, Fig. S9). Consistent with this effect on STAT activation, both LY294002 and Wortmannin suppressed increased CXCL10 secretion by CAV1-silenced PAECs (Fig. 7*B*). Next, two currently available antitumor drugs, a pan-PI3K inhibitor (GDC-0980) and a pan-AKT inhibitor (MK-2206), were used to examine the contribution of PI3K/AKT activation to CAV1 deficiency-induced proliferation. Both inhibitors attenuated proliferation in CAV1-silenced PAECs (Fig. 7*C*) and concurrent inhibition of $pAKT^{Ser473}$ by GDC-0980 is shown in Fig. 7*D*. Collectively, these results suggest that STAT and AKT activation may contribute to the proliferative and IFN-biased inflammatory phenotype of CAV1-silenced PAECs. However, unlike JAK/STAT inhibitors, PI3K/AKT blockade was able to shut down both pathways and warrants further investigation as a strategy for treating the disease-defining vascular remodeling of PAH.

NOS3 Knockdown Prevents Constitutive STAT1 and AKT Activation in CAV1-Deficient Human PAECs. Endothelial dysfunction associated with reduced CAV1 expression has been previously linked to dysregulated NOS3 activity (5, 34–36). In particular, under conditions that promote NOS3 uncoupling (e.g., depletion of CAV1, L-arginine, and tetrahydrobiopterin), phosphorylation at serine 1177 (Ser1177) by AKT increases superoxide production, thereby favoring production of peroxynitirite, a potent mediator of intracellular oxidant stress (36, 37). Therefore, we next examined whether Ser1177 phosphorylation of NOS3 was altered in CAV1-silenced PAECs. In line with prior studies (5, 38), NOS3 phosphorylation at ser1177 was significantly increased in CAV1-deficient PAECs (Fig. 8*A*), consistent with our finding of constitutive AKT activation. Furthermore, *NOS3* gene silencing abrogated both constitutive STAT1 and AKT activation (Fig. 8 *B* and *C*), evoking NOS3 uncoupling as potential contributor to IFN activation in CAV1-silenced human PAECs.

Exogenous IFN Decreases CAV1 Expression and Mirrors CAV1 Loss-Induced Alteration of the Cytoskeletal Architecture in Human PAECs. Since CAV1 loss induced inflammatory adhesion molecules and IFN target genes, human PAECs were treated with exogenous IFN-α (100 U/mL) (39), IFN-β (10 ng/mL) (40), and IFN-γ (1,000 ng/mL) (41) using previously published doses for endothelial cell cultures, to determine their effects on CAV1 expression, JAK/STAT and AKT signaling, as well as cellular phenotype. As expected, all three IFNs activated STAT1, as determined by phosphorylation, and increased STAT1 expression (*SI Appendix*, Fig. S10*A*). Challenging human PAECs with either type I or type II IFNs substantially decreased *CAV1* protein (Fig. 8*D*), while mean *CAV1* mRNA expression was not significantly suppressed by either IFN-α or -β. Somewhat differently, IFN-γ treatment nominally decreased *CAV1* mRNA levels (*SI Appendix*, Fig. S10*B*). AKT was also activated in response to IFN exposure (Fig. 8*E*), similar to CAV1 silencing in these cells. Furthermore, immunofluorescence staining revealed attenuation of central stress fibers (Fig. 8*F*), albeit less pronounced than in

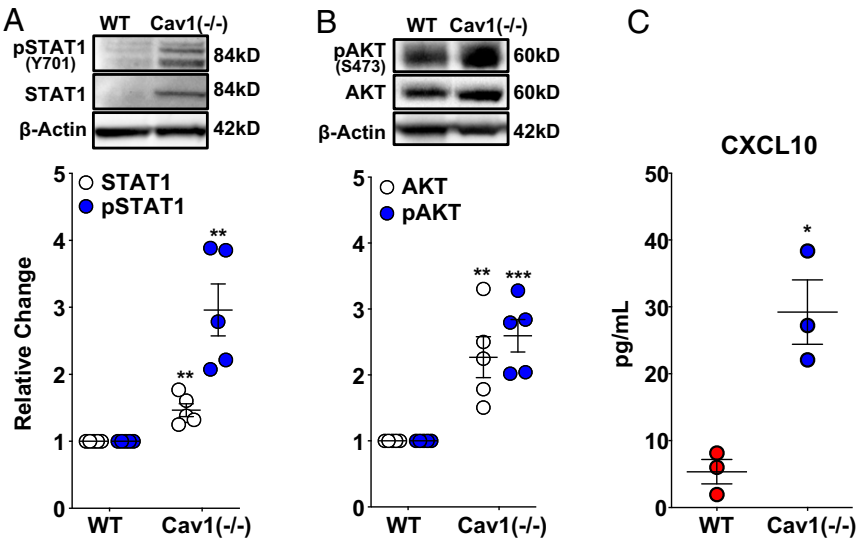

Fig. 4. Activation of STAT/AKT signaling and CXCL10 production in *Cav1*$^{-/-}$ mice replicates CAV1 loss in primary human PAECs. (*A*) Total and phosphorylated (activated) STAT1 and (*B*) total and phosphorylated (activated) AKT were significantly increased in Cav1-null mice compared to wild-type controls. Densitometric quantification of protein normalized to β-actin presented relative to wild-type controls as mean ± SE, along with representative Western blots. (*C*) Circulating CXCL10 measured by ELISA (mean ± SE) was significantly increased in *Cav1*$^{-/-}$ mice compared to wild-type controls. *$P < 0.05$, **$P < 0.01$, ***$P < 0.001$.

CAV1-silenced PAECs where CAV1 protein levels are more markedly reduced. These findings raise the possibility that IFN itself can induce a PAH-like, dysfunctional PAEC phenotype with CAV1 loss that in turn may further augment downstream JAK/STAT and AKT signaling.

Discussion

Using an in vitro model of *CAV1* gene silencing in human PAECs, we demonstrated that CAV1 plays a crucial role in protecting human pulmonary arterial endothelial cells from excessive proliferation, apoptosis resistance, hypermigration, and inflammation. Importantly, the phenotypic abnormalities caused by CAV1 knockdown were closely mirrored by dermal fibroblasts from HPAH patients with a CAV1 loss-of-function mutation. Moreover, the inflammatory component of these anomalous attributes was surprisingly specific, consisting of STAT and AKT activation and a predominant type I IFN-driven gene signature, as demonstrated by global expression profiling. CAV1-null mice and blood CXCL10 levels in HPAH patients with *CAV1* mutations confirmed the presence of a constitutively activated IFN inflammatory response in vivo. In vitro, JAK/STAT inhibitors blocked many of the phenotypic features of CAV1 loss in human PAECs but did not dampen AKT activation. In contrast, blocking aberrant AKT activation not only mitigated functional and phenotypic abnormalities caused by CAV1 deficiency in PAECs, but also suppressed STAT activation and secretion of CXCL10, an archetypal IFN target gene. Collectively, these findings demonstrate that CAV1 loss, either from mutations or suppression by other mechanisms in IPAH, can result in aberrant endothelial type I IFN activation. Importantly, type I (IFN-α and IFN-β) or type II IFN (IFN-γ) stimulation was sufficient to reduce the expression of CAV1 protein, induce both STAT1 and AKT activation, and disrupt the cytoskeletal organization of human PAECs. These findings have implications for understanding mechanisms by which autoimmune and autoinflammatory diseases (24, 25), as well as IFN therapy (22), all lead to PAH. Furthermore, JAK/STAT and AKT signaling warrant further investigation as potential therapeutic targets for arresting or even possibly reversing pathologic vascular remodeling in CAV1 loss-associated PAH.

Enhanced cell proliferation in CAV1-silenced PAECs is consistent with previous findings, which conversely showed that CAV1 overexpression caused cell cycle arrest at G0/G1 phase in endothelial cells (42, 43). Furthermore, dermal fibroblasts from HPAH patients harboring a heterozygous c.474delA frameshift mutation displayed a proproliferative phenotype analogous to CAV1-silenced PAECs, confirming the results of a recent study using the same cells (44). Investigations of CAV1 expression and function in endothelial cells (45) and its role in PAH pathogenesis (46) have reported variable effects on proliferation, migration, and angiogenesis, depending on experimental conditions and cell type (47–50). Here, a proliferative, hypermigratory phenotype resulted from either molecular (siRNA gene silencing in PAECs) or genetic (fibroblasts expressing a pathogenic CAV1 mutation) disruption of CAV1 expression. Notably, closure of a monolayer defect in vitro likely reflects both proliferation and migration of CAV1-deficient cells (51). While attenuation of well-formed stress-fibers as seen in our CAV1-silenced PAECs, might support aspects of an undirected migratory phenotype, coherent, directional migration has been reported to be impaired by CAV1 loss (47). Importantly, altered VE-cadherin and PECAM-1 expression and localization in CAV1-deficient PAECs is consistent with prior work that found increased lung vascular permeability in *Cav1*$^{-/-}$ mice, a defect that was reversed by endothelial-specific CAV1 reconstitution (13). Similarly, CAV1 knockdown was previously shown to hamper insulin-induced actin remodeling in bovine aortic endothelial cells (52).

Notably, while CAV1 protein expression is reduced in PAH lung samples (5–7, 35), mRNA transcript levels have been more inconsistent. While an early microarray study revealed significantly decreased CAV1 mRNA expression in whole lung tissue from PAH patients (53), a more recent study found that CAV1 mRNA expression was increased in isolated PAECs from PAH patients (5). Here we demonstrate that stimulation of PAECs with exogenous IFNs reduced CAV1 protein with variable effects on *CAV1* mRNA levels. Importantly, the reduction of CAV1 protein expression in the absence of a significant decrease in mRNA levels following IFN-α and IFN-β exposure is consistent with previously reported mechanisms of CAV1 protein loss that were independent of gene transcription (5, 6). Nevertheless, Interferome 2.01, a

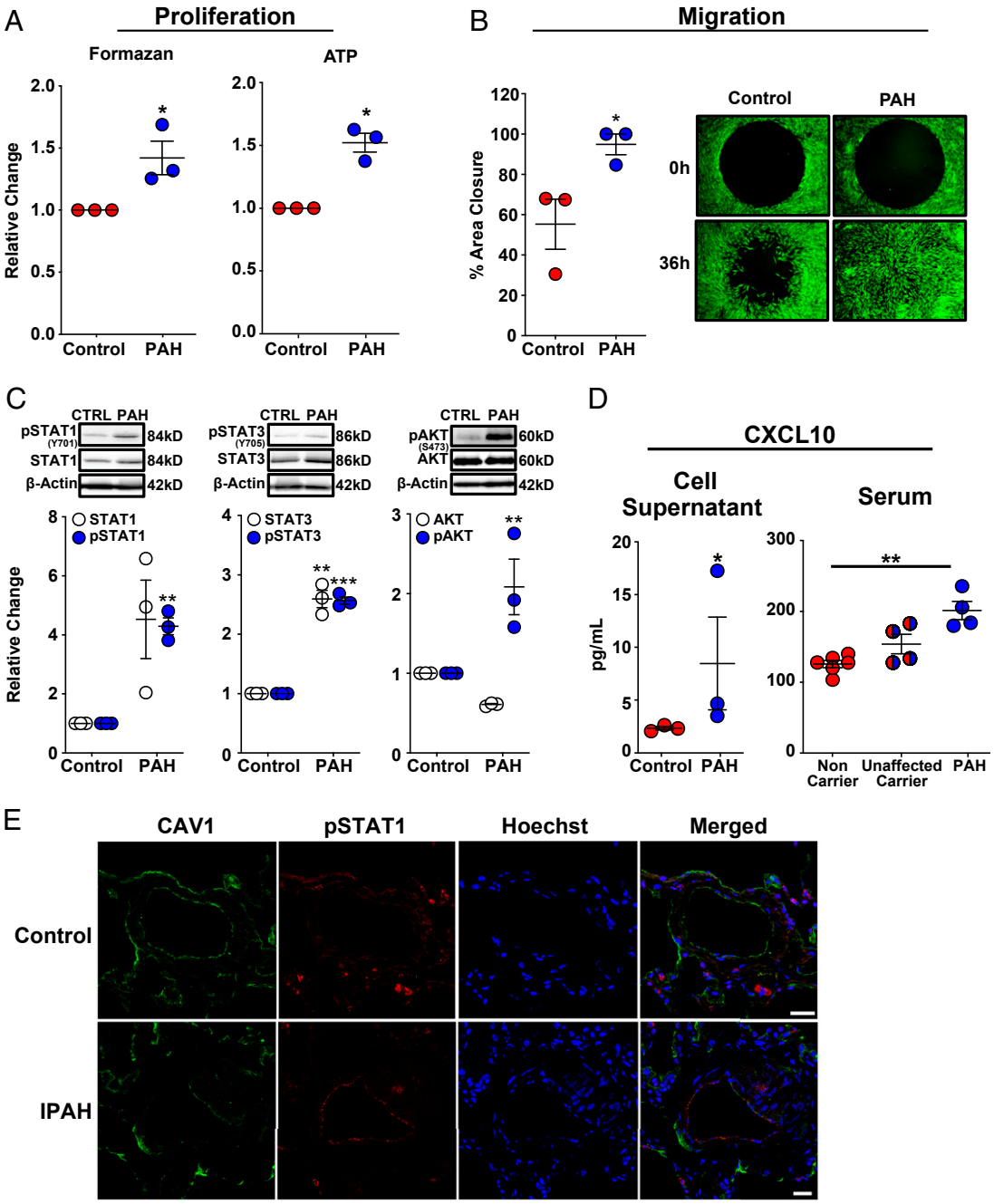

Fig. 5. Dermal fibroblasts from patients with HPAH and the endothelial layer of distal pulmonary arterioles in patients with IPAH mirror CAV1-silenced primary human PAECs. (*A*) Dermal fibroblasts with a HPAH-associated *CAV1* mutation demonstrated enhanced proliferation as assessed by MTS and ATP assays. Fibroblasts were seeded in 96-well plates in complete media for 6 h, then serum-starved for 24 h, followed by return to complete media for 72 h to assess proliferation. Data presented as mean FC ± SE. (*B*) Cell migration was significantly increased in CAV1-mutant fibroblasts from HPAH patients compared to healthy control fibroblasts. Fibroblasts were seeded in 96-well plates containing a circular gel insert (Oris Pro Cell Migration Assay) and allowed to adhere for 6 h. Cells were then serum-starved for 24 h, returned to complete media and the insert was removed. Percent closure of the monolayer defect was assessed 36 h later. Data presented as mean ± SE. A representative image at 0 and 36 h is shown (*Right*; 10× magnification). (*C*) CAV1-mutant fibroblasts from HPAH patients demonstrated a significant increase in phosphorylated (activated) STAT1, STAT3, and AKT^{Ser473}. Similarly, there was a trend toward an increase in total STAT1 expression ($P = 0.06$) and a significant increase in total STAT3. Phosphorylated and total STAT1 and STAT3 expression, as well as phosphorylated and total AKT, are normalized to β-actin. Densitometric quantification presented relative to control fibroblasts as mean ± SE, along with representative Western blots. (*D*) CAV1-mutant fibroblasts produced significantly higher concentrations of CXCL10 compared to control fibroblasts. CXCL10, measured by ELISA in cell supernatants after 48 h presented as mean ± SE. Replication used dermal fibroblasts from unique HPAH patients and healthy controls. HPAH patients harboring the identical *CAV1* mutation (c.474delA) as the fibroblasts above had significantly higher serum CXCL10 concentrations than noncarriers. Notably, unaffected carriers of the CAV1 gene variant had a trend toward higher serum CXCL10 concentrations compared to noncarriers ($P = 0.06$), but similar levels compared to mutation carriers with HPAH ($P = 0.29$). CXCL10 was measured by ELISA and quantified based on a standard curve. Serum was available from two of the three HPAH patients that also provided dermal fibroblasts and two additional HPAH patients from PAH Biobank. $^*P < 0.05$, $^{**}P < 0.01$, $^{***}P < 0.001$. (*E*) Immunofluorescence staining revealed CAV1 (green) loss and STAT1 (red) activation in distal PAECs of IPAH patients ($n = 5$) compared to control lung samples ($n = 5$). Cell nuclei (blue) are stained with Hoechst 33342. (Scale bars, 25 μm.) Representative images are shown.

database of IFN regulated genes, includes CAV1 among IFN-suppressed genes, similar to our findings in IFN-γ–treated PAECs.

In addition to angioproliferative vascular remodeling, lung histopathology from PAH patients is notable for perivascular inflammatory cell infiltrates (54, 55), which presumably could be recruited to plexiform lesions by a dysfunctional, proinflammatory pulmonary vascular endothelium. Importantly, CAV1 knockdown in PAECs induced expression of adhesion molecules (ICAM1 and VCAM1) and cytokines (IL-6 and IL-8), proinflammatory molecules that have been directly linked to PAH pathogenesis (56), as well as type I interferonopathies (24, 25). Genome-wide expression profiling of CAV1-silenced PAECs identified a predominant type I IFN signature, further supporting the proinflammatory endothelial phenotype we observed. Accordingly, CAV1 loss appeared to derepress inflammatory activation, and specifically IFN responses, in endothelial cells. CXCL10, a classic IFN target gene whose expression was increased in CAV1-silenced PAECs, has been shown to prime T lymphocyte adhesion to endothelium (57), stimulate $CXCR3^+$ T cell migration to the lung, and is up-regulated in the serum of PAH patients (58). Furthermore, among the differentially expressed IFN target genes identified by microarray, both *CCL2* and *CCL5* mRNA were significantly up-regulated. This finding is consistent with previously reported elevated levels of CCL2 in serum and lung tissue of IPAH patients, as well as increased CCL2 secretion by PAH lung-derived endothelial cells (59). Similarly, *CCL5* mRNA expression is elevated in PAH lung tissue and CCL5 protein expression is specifically increased in the endothelial cells of remodeled precapillary pulmonary arteries (60). The IFN predominant inflammatory response that results from CAV1 depletion demonstrated here, along with previous evidence that endothelial CAV1 expression, is reduced by inflammatory mediators—such as TNF-α (5), LPS, and IL-6 (34)—suggests the potential for a feed-forward mechanism that sustains chronic inflammation in PAH.

Given the IFN-biased gene signature, it is not surprising that another prominent feature of global transcriptomic changes in CAV1-silenced PAECs was evidence of an antiviral response. Mirroring gene-expression changes observed in CAV1-deficient PAECs, metaanalysis of blood transcriptomic studies recently demonstrated a prominent, IFN-driven gene signature in the circulating cells of PAH patients that was similarly enriched for antiviral response genes (61). Interestingly, a recent study detailed the potential pathogenic role of an endogenous retrovirus (ERV) as a trigger for inflammatory vessel remodeling in PAH (62). Notably, *ERV3* was among the differentially expressed, up-regulated transcripts identified by microarray in CAV1-silenced PAECs. ERV3 has been proposed to act as an autoantigen involved in various immune-pathologies (63). While ERV3-encoded gene products have been shown to result in both immunosuppressive (64) as well as immunostimulatory (65) effects, CAV1 deficiency may predispose to an exaggerated IFN-mediated inflammatory response to viral gene products.

Induction of JAK/STAT signaling as a consequence of CAV1 gene silencing is consistent with evidence linking reduced CAV1 expression in psoriatic plaques to enhanced cytokine production and keratinocyte hyperproliferation through JAK/STAT activation (19). It is important to emphasize that CAV1-silencing in PAECs

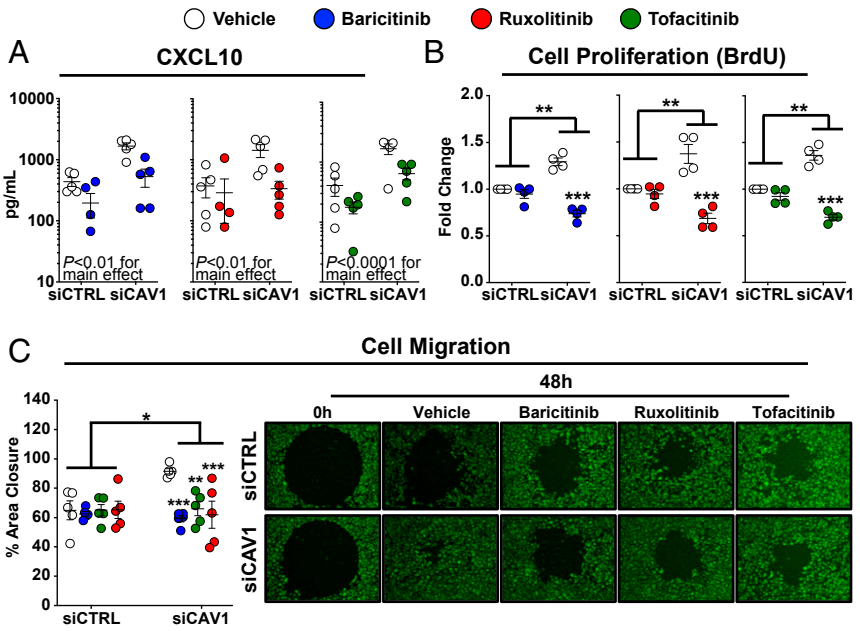

Fig. 6. JAK/STAT inhibitors block IFN activation, proliferation, and migration in CAV1-deficient primary human PAECs but fail to reduce constitutive AKT activation. (*A*) CXCL10 protein was reduced by baricitinib (100 nM), ruxolitinib (100 nM), or tofacitinib (100 nM) in both CAV1-silenced and siCTRL treated PAECs. After siRNA transfection (48 h), PAECs were serum-starved for 24 h followed by 24 h of drug treatment or vehicle control prior to cell supernatant collection. CXCL10 concentration, measured by ELISA, presented as mean ± SE. (*B*) Treatment with baricitinib (100 nM), ruxolitinib (100 nM), and tofacitinib (100 nM) all reduced cell proliferation, as assessed by bromodeoxyuridine (BrdU) incorporation, in CAV1-silenced PAECs. BrdU incorporation was unaffected in siCTRL transfected PAECs treated with either baricitinib, ruxolitinib, or tofacitinib ($P \geq 0.20$ for all compared to vehicle-treated siCTRL cells). After CAV1 knockdown (48 h), PAECs were transferred to 96-well plates in complete media for 6 h, then serum-starved for 24 h and returned to complete media with the specified JAK/STAT inhibitor or vehicle control. BrdU was added after 48 h of drug treatment and incorporation was assessed 24 h later. Data presented as mean FC ± SE. (*C*) Treatment with baricitinib (100 nM), ruxolitinib (100 nM), or tofacitinib (100 nM) significantly reduced cell migration in CAV1-silenced PAECs ($P = 0.02$ for the interaction between CAV1-silencing and drug treatment). After CAV1 knockdown (48 h), PAECs were transferred to 96-well plates containing a circular gel insert (Oris Pro Cell Migration Assay) for 6 h, then serum-starved for 24 h, followed by return to complete media with the specified JAK/STAT inhibitor or vehicle control and the insert was removed. Percent closure of the monolayer defect was assessed 48 h later. Data presented as the mean ± SE with representative images at 0 and 48 h shown (*Right*; 10× magnification). Replication throughout represent independent experiments each using different PAEC donors. $*P < 0.05$, $**P < 0.01$, $***P < 0.001$.

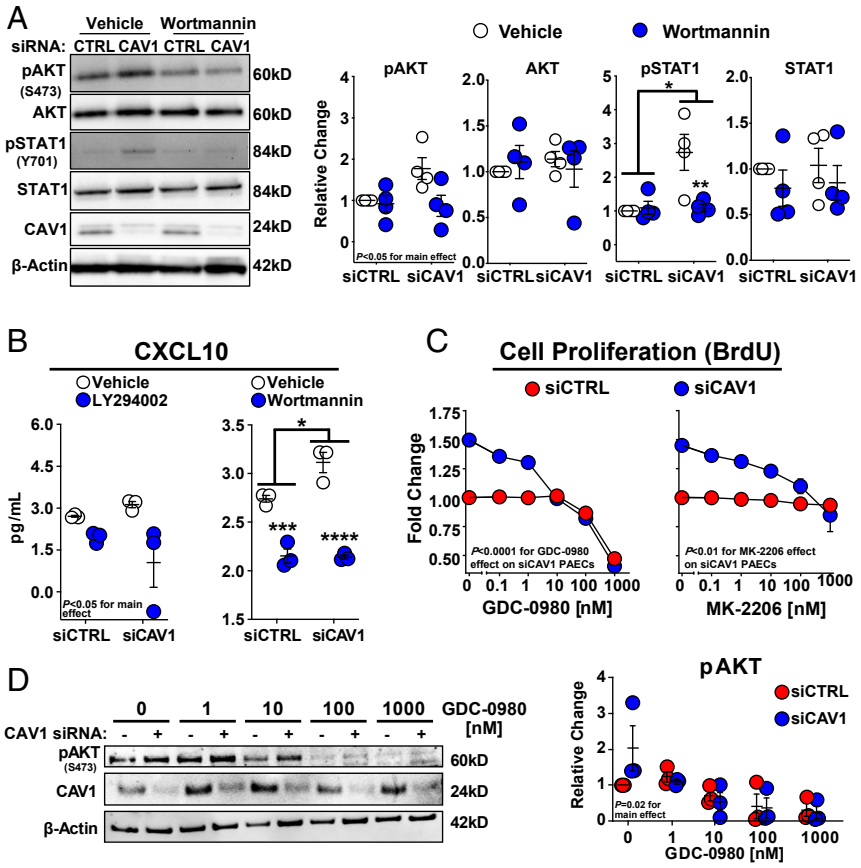

Fig. 7. PI3K/AKT inhibitors block AKT and STAT1 activation blunting induction of the IFN response, proliferation and migration in CAV1-deficient primary human PAECs. (*A*) Treatment with Wortmanin (50 nM) significantly reduced AKT activation in PAECs with a trend for this effect to be larger in CAV1-silenced cells than siCTRLs ($P = 0.06$; for an interaction). Wortmanin also significantly reduced STAT1 activation in CAV1-deficient PAECs with no effect on siCTRL cells. Total AKT or STAT1 were not altered by Wortmanin ($P \geq 0.10$). Densitometric quantification of phosphorylated and total AKT and STAT1 is normalized to β-actin and presented relative to vehicle-treated siCTRLs (mean ± SE) with representative Western blots displayed on the left. (*B*) CXCL10 production was reduced by LY294002 and Wortmanin in both CAV1-silenced and siCTRL transfected PAECs. CXCL10 measured by ELISA presented as mean± SE. After siRNA transfection (48 h), PAECs were serum-starved for 24 h followed by 24 h of drug treatment or vehicle control prior to whole-cell lysate or cell supernatant collection. (*C*) Both GDC-0980 and MK-2206, PI3K/AKT inhibitors, dose-dependently reduced cell proliferation in CAV1-silenced PAECs. Unlike GDC-0980, which reduced cell proliferation of siCTRL PAECs at high doses ($P < 0.0001$ for the downward trend of the slope at doses >10 nM), MK-2206 treatment did not impact proliferation in siCTRL cells ($P = 0.51$ for the slope). After CAV1 knockdown (48 h), PAECs were transferred to 96-well plates in complete media for 6 h. Cells were then serum-starved for 24 h, returned to complete media, and then treated with either GDC-0980, MK-2206, or vehicle control. BrdU was added after 48 h of drug treatment and incorporation was assessed 24 h later. Data for GDC-0980 ($n = 4$) and MK-2206 ($n = 3$) is presented as the mean FC ± SE. (*D*) Treatment with a pan-PI3K inhibitor (GDC-0980) reduced $pAKT^{Ser473}$ in both CAV1-silenced PAECs and siCTRLs. After siRNA transfection (48 h), PAECs were treated with drug or vehicle control for 6 h prior to whole-cell lysate collection. Representative Western blot shown from three experiments. Replication throughout represents independent experiments each using different PAEC donors. *$P < 0.05$, **$P < 0.01$, ***$P < 0.001$, ****$P < 0.0001$.

led to the induction of an IFN inflammatory gene response both in the absence and presence of exogenous IFN stimulation. The predominance of this response was specific for CAV1 knockdown and was not seen with control siRNA or in our model of BMPR2-silenced PAECs (66). Nonetheless, induction of IFN-like responses has been reported with siRNA exposure in a length, concentration, GU-content, and cell-type–dependent manner, and thus may not be generalizable across different experiments. However, the CAV1-specific siRNA used here was only 19-bp long, which is shorter than the length of oligonucleotides associated with IFN induction (21 to 23 bp) and the GU-content was also much less than the pooled control siRNAs (26% versus a mean of 53%). The activation of STAT in mouse lung homogenates and concurrent increases in serum CXCL10 concentrations strongly supports our in vitro findings in CAV1-silenced PAECs and further argues against off-target effects due to siRNA. IFN-α, IFN-β, and CXCL10 production was associated with the downstream activation of IRF3, IRF7, STAT1, and STAT3, as well as increased total STAT1, which was shown to prolong the expression of a subset of IFN-induced genes (67, 68). Notably, STAT3 has been implicated in the proliferative and fibrotic response to CAV1 deficiency (69) and in the pathogenesis of PAH (70).

However, this study demonstrates STAT1 activation due to CAV1 loss. Since normal cell viability is not dependent on STAT1 activity (71), STAT1 might be a relatively safe therapeutic target for reversing proliferative vascular remodeling in PAH. While IFN-responsive genes have been classically linked to growth inhibition, senescence, and apoptosis (72, 73), our findings correspond more closely to recent studies that link STAT1 activation to proliferation (74, 75), possibly indicating a more complex and nuanced role for the regulation of cell growth by IFNs. Here we demonstrated that currently available, FDA-approved JAK/STAT pathway inhibitors (baricitinib, ruxolitinib, tofacitinib) not only blocked STAT1 activation and CXCL10 expression, but also blunted proliferation and migration in CAV1-silenced PAECs. IFN-driven responses could also be targeted more proximally with

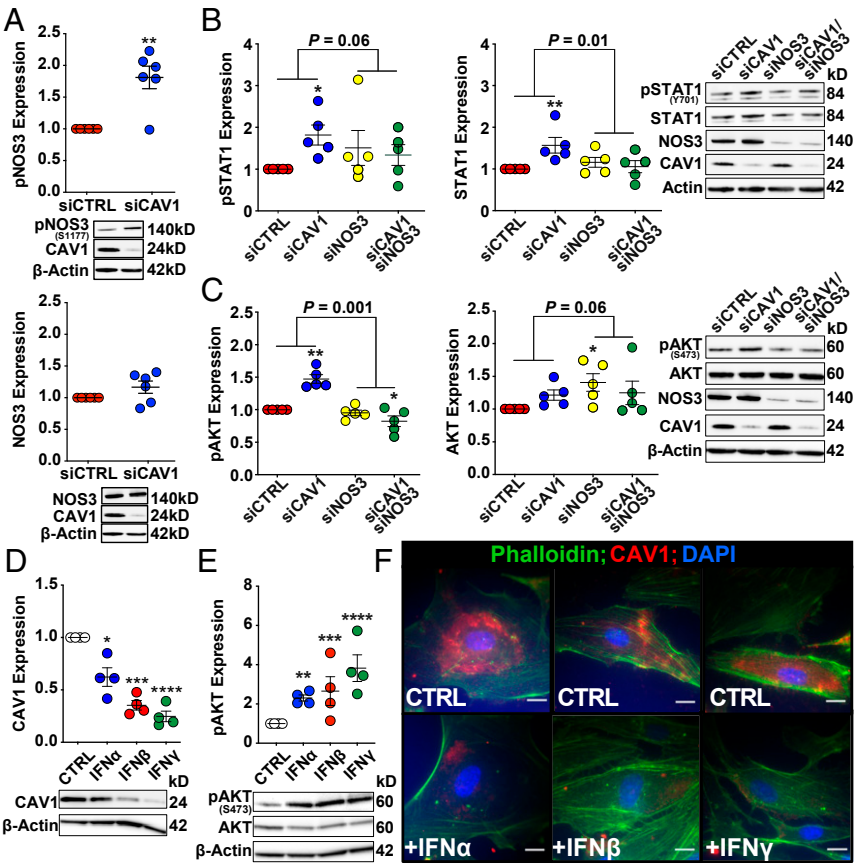

Fig. 8. Knockdown of NOS3 prevents constitutive activation of STAT1 and AKT in *CAV1*-silenced cells and exogenous IFN treatment decreases CAV1 expression, activates AKT, and disrupts cytoskeletal architecture in primary human PAECs. (*A*) NOS3 is activated (phosphorylated at Ser1177) in CAV1-deficient PAECs while total NOS3 expression is unchanged compared to siCTRL transfected cells ($P = 0.19$). Whole-cell lysates were collected 48 h following siRNA transfection and protein levels were assess by immunoblotting. The effect of CAV1 loss on phosphorylated (activated) and total (*B*) STAT1 and (*C*) AKT levels were significantly different in the presence and absence of *NOS3* knockdown. $^{*}P < 0.05$, $^{**}P < 0.01$, for the comparison with siCTRL. An interaction between siCAV1 and siNOS3 conditions was considered significant at $P < 0.10$. Treatment of PAECs with either IFN-α (100 IU/mL), IFN-β (10 ng/mL), or IFN-γ (1,000 ng/mL) (*D*) reduced CAV1 protein expression, as well as (*E*) increased phosphorylated (activated) AKT. PAECs were serum-starved for 24 h followed by treatment with IFN-α, IFN-β, IFN-γ, or vehicle alone for 24 h prior to cell lysate collection. Densitometric quantification of protein, normalized to β-actin and relative to vehicle treated PAECs, is presented as mean ± SE and representative Western blots are shown. Replication represents independent experiments each using different PAEC donors. $^{*}P < 0.05$, $^{**}P < 0.01$, $^{***}P < 0.001$, $^{****}P < 0.0001$ for the comparison vehicle control. (*F*) Immunofluorescence staining of PAECs treated with IFN-α (100 IU/mL), IFN-β (10 ng/mL), or IFN-γ (1,000 ng/mL) for 24 h demonstrated reduced CAV1 expression (red) and disruption in well-formed filamentous actin (Phalloidin; green). Nuclei are stained blue with DAPI. Images are representative of three independent experiments, each with a different donor. (Scale bar, 20 μm.)

monoclonal antibodies that directly inhibit the IFN-α/β receptor (76), a concept that was not tested here. Notably, in patients with myelofibrosis, JAK/STAT inhibitor therapy has sometimes improved (31) and at other times worsened (32) concomitant pulmonary hypertension, suggesting that incompletely understood factors may affect the efficacy of this approach.

Caveolae, through the scaffolding functions of CAV1, negatively regulate many signaling cascades critical for cell proliferation, migration, and apoptosis, such as the mitogen-activated protein kinase (MAPK) and AKT pathways (13). We observed activation of AKT but not ERK in CAV1-silenced PAECs, consistent with previous findings in CAV1-silenced bovine aortic endothelial cells (12). Importantly, STAT1 and STAT3 phosphorylation, and therefore activation, can be mediated by PI3K/AKT directly, independent of JAK (77, 78). Similarly, AKT activation complements and reinforces STAT signaling by promoting the translation of IFN-stimulated genes (20). Therefore, although a precise mechanistic link between CAV1 loss and constitutive IFN activation is yet to be determined, loss of CAV1 undoubtedly impedes its normal functions, including molecular scaffolding, trafficking, and signal transduction. For example, consistent with prior studies (5, 38), we found that NOS3 Ser1177 phosphorylation is increased in CAV1-deficient PAECs and that NOS3 knockdown decreased both constitutive STAT1 and AKT activation. Thus, the disruption of CAV1 and NOS3 regulatory coupling appears, at least in part, to contribute to the activation of STAT and AKT signaling with the downstream induction of an IFN inflammatory response.

Constitutive activation of STAT/AKT and evidence of a type I IFN response in CAV1-silenced PAECs was similarly demonstrated in vitro using HPAH patient fibroblasts expressing a pathogenic CAV1 gene variant, as well as in lung tissue and blood from *Cav1* knockout mice. Perhaps more importantly, endothelial CAV1 loss and STAT1 activation was found in the small pulmonary arteries of patients with idiopathic PAH, indicating that this inflammatory phenotype might be more widely applicable and not merely limited to the very few patients harboring rare CAV1 frameshift mutations. While JAK/STAT inhibitors did not block AKT phosphorylation, two different PI3K inhibitors significantly diminished both AKT and STAT1 activation in CAV1-deficient PAECs. Furthermore, two orally active antitumor therapies, targeting PI3K/mTOR (mammalian target

of rapamycin; GDC-0980) or AKT (MK-2660) dose-dependently reduced CAV1-silenced PAEC proliferation at concentrations achievable in patients. Constitutive Smad1/5/8 phosphorylation was recently observed in the same dermal fibroblasts from HPAH patients investigated here, and use of a chemical inhibitor of ALK1/2/3/6 reduced cell proliferation in these CAV1 mutant cells, suggesting that other growth-promoting pathways may also be involved (44).

In conclusion, comprehensive in vitro characterization of CAV1 deficiency in PAECs revealed a proliferative, IFN-biased inflammatory phenotype driven by constitutively activated STAT and AKT signaling. While JAK/STAT and PI3K/AKT inhibitors similarly mitigated inflammation and proliferation, only PI3K/AKT inhibitors blocked both aberrantly activated pathways simultaneously. Based on strong preclinical data (79), mTOR inhibition downstream from PI3K/AKT is currently under investigation in PAH patients (NCT02587325). Determining if PAH-associated signaling abnormalities can be safely targeted more proximally and whether such an approach might yield greater benefits in addressing pathologic vascular remodeling warrants further study.

Materials and Methods

Detailed descriptions are provided in *SI Appendix*.

Dermal Fibroblasts and Serum Samples from HPAH Patients. The Office of Human Subjects Research Protections approved the use of deidentified dermal fibroblasts (*SI Appendix*, Table S2) and serum from HPAH patients (*SI Appendix*, Table S3) with known CAV1 mutations and controls provided by Vanderbilt University (OHSRP no. 13084), as well as the use of deidentified serum samples from the National Biological Sample and Data Repository for PAH (*SI Appendix*, Table S3) (OHSRP no. 18-CC-00542). The institutional review board of Vanderbilt University approved the clinical protocol originally associated with their samples (#9401). All participants provided written informed consent.

***Cav1*$^{-/-}$ Mice.** All aspects of animal testing and care were approved by the NIH Clinical Center Animal Care and Use Committee and conducted in accordance with the NIH *Guidelines for the Care and Use of Laboratory Animals* (80).

Microarray Expression Analysis. Raw and RMA normalized data were submitted to the National Center for Biotechnology Information Gene Expression Omnibus database (NCBI GEO; https://www.ncbi.nlm.nih.gov/projects/geo/index.cgi; accession no. GSE138991), and all data are MIAME compliant.

Statistical Analysis. Statistical analysis was performed using JMP version 12.1 (SAS Institute) with a two-tailed α of 0.05 as the cut-off for significance. Data are represented as arithmetic means $\pm$ SE except mRNA levels measured by qRT-PCR, for which geometric means of FCs were plotted.

Data Availability. Raw and RMA normalized data were submitted to the NCBI GEO database, https://www.ncbi.nlm.nih.gov/projects/geo/index.cgi (accession no. GSE138991). All other study data are included in the article and supporting information.

ACKNOWLEDGMENTS. We thank Lynne Holtzclaw at the Microscopy & Imaging Core Facility (National Institute of Child Health and Human Development, NIH) for instrumental support with confocal imaging; Kelly Byrne for assistance with editing and formatting the manuscript and figures; and contributors, including the pulmonary hypertension centers who collected samples used in this study, as well as patients and their families, whose help and participation made this work possible. Samples and data from the National Biological Sample and Data Repository for Pulmonary Aterial Hypertension, which receives government support under investigator-initiated Grant R24 HL105333 awarded by the National Heart Lung and Blood Institute, were used in this study. Tissue samples used in this study were provided by the Pulmonary Hypertension Breakthrough Initiative (PHBI) Network. Funding for the PHBI is provided under a National Heart Lung and Blood Institute R24 grant, HL123767, and by the Cardiovascular Medical Research and Education Fund (CMREF). This study was funded by intramural funds from the National Institute of Health Clinical Center. The opinions expressed in this article are those of the authors and do not represent any position or policy of the NIH, the US Department of Health and Human Services, or the US Government.

1. S. Sakao, K. Tatsumi, N. F. Voelkel, Endothelial cells and pulmonary arterial hypertension: Apoptosis, proliferation, interaction and transdifferentiation. *Respir. Res.* **10**, 95 (2009).
2. N. Galiè *et al.*, Risk stratification and medical therapy of pulmonary arterial hypertension. *Eur. Respir. J.* **53**, 1801889 (2019).
3. Y. C. Lai, K. C. Potoka, H. C. Champion, A. L. Mora, M. T. Gladwin, Pulmonary arterial hypertension: The clinical syndrome. *Circ. Res.* **115**, 115–130 (2014).
4. E. D. Austin *et al.*, Whole exome sequencing to identify a novel gene (caveolin-1) associated with human pulmonary arterial hypertension. *Circ. Cardiovasc. Genet.* **5**, 336–343 (2012).
5. F. R. Bakhshi *et al.*, Nitrosation-dependent caveolin 1 phosphorylation, ubiquitination, and degradation and its association with idiopathic pulmonary arterial hypertension. *Pulm. Circ.* **3**, 816–830 (2013).
6. S. D. S. Oliveira *et al.*, Injury-induced shedding of extracellular vesicles depletes endothelial cells of Cav-1 (caveolin-1) and enables TGF-β (transforming growth factor-β)-dependent pulmonary arterial hypertension. *Arterioscler. Thromb. Vasc. Biol.* **39**, 1191–1202 (2019).
7. R. O. Achcar *et al.*, Loss of caveolin and heme oxygenase expression in severe pulmonary hypertension. *Chest* **129**, 696–705 (2006).
8. K. G. Rothberg *et al.*, Caveolin, a protein component of caveolae membrane coats. *Cell* **68**, 673–682 (1992).
9. R. G. Parton, M. A. del Pozo, Caveolae as plasma membrane sensors, protectors and organizers. *Nat. Rev. Mol. Cell Biol.* **14**, 98–112 (2013).
10. M. Ramos, M. W. Lamé, H. J. Segall, D. W. Wilson, The BMP type II receptor is located in lipid rafts, including caveolae, of pulmonary endothelium in vivo and in vitro. *Vascul. Pharmacol.* **44**, 50–59 (2006).
11. C. Wunderlich *et al.*, The adverse cardiopulmonary phenotype of caveolin-1 deficient mice is mediated by a dysfunctional endothelium. *J. Mol. Cell. Cardiol.* **44**, 938–947 (2008).
12. E. Gonzalez, A. Nagiel, A. J. Lin, D. E. Golan, T. Michel, Small interfering RNA-mediated down-regulation of caveolin-1 differentially modulates signaling pathways in endothelial cells. *J. Biol. Chem.* **279**, 40659–40669 (2004).
13. T. Murata *et al.*, Reexpression of caveolin-1 in endothelium rescues the vascular, cardiac, and pulmonary defects in global caveolin-1 knockout mice. *J. Exp. Med.* **204**, 2373–2382 (2007).
14. N. P. Nickel *et al.*, Elafin reverses pulmonary hypertension via caveolin-1-dependent bone morphogenetic protein signaling. *Am. J. Respir. Crit. Care Med.* **191**, 1273–1286 (2015).
15. X. Nie *et al.*, CCL5 deficiency rescues pulmonary vascular dysfunction, and reverses pulmonary hypertension via caveolin-1-dependent BMPR2 activation. *J. Mol. Cell. Cardiol.* **116**, 41–56 (2018).
16. M. Drab *et al.*, Loss of caveolae, vascular dysfunction, and pulmonary defects in caveolin-1 gene-disrupted mice. *Science* **293**, 2449–2452 (2001).
17. B. Razani *et al.*, Caveolin-1 null mice are viable but show evidence of hyperproliferative and vascular abnormalities. *J. Biol. Chem.* **276**, 38121–38138 (2001).
18. S. Minguet *et al.*, Caveolin-1-dependent nanoscale organization of the BCR regulates B cell tolerance. *Nat. Immunol.* **18**, 1150–1159 (2017).
19. Y. Yamaguchi, Y. Watanabe, T. Watanabe, N. Komitsu, M. Aihara, Decreased expression of caveolin-1 contributes to the pathogenesis of psoriasiform dermatitis in mice. *J. Invest. Dermatol.* **135**, 2764–2774 (2015).
20. S. Kaur *et al.*, Role of the Akt pathway in mRNA translation of interferon-stimulated genes. *Proc. Natl. Acad. Sci. U.S.A.* **105**, 4808–4813 (2008).
21. C. Oh *et al.*, A central role for PI3K-AKT signaling pathway in linking SAMHD1-deficiency to the type I interferon signature. *Sci. Rep.* **8**, 84 (2018).
22. L. Savale *et al.*, Pulmonary arterial hypertension in patients treated with interferon. *Eur. Respir. J.* **44**, 1627–1634 (2014).
23. R. B. Christmann *et al.*, Interferon and alternative activation of monocyte/macrophages in systemic sclerosis-associated pulmonary arterial hypertension. *Arthritis Rheum.* **63**, 1718–1728 (2011).
24. A. Brehm *et al.*, Additive loss-of-function proteasome subunit mutations in CANDLE/PRAAS patients promote type I IFN production. *J. Clin. Invest.* **126**, 795 (2016).
25. Y. Liu *et al.*, Activated STING in a vascular and pulmonary syndrome. *N. Engl. J. Med.* **371**, 507–518 (2014).
26. B. Ranchoux *et al.*, Endothelial-to-mesenchymal transition in pulmonary hypertension. *Circulation* **131**, 1006–1018 (2015).
27. A. Reynolds *et al.*, Induction of the interferon response by siRNA is cell type- and duplex length-dependent. *RNA* **12**, 988–993 (2006).
28. C. Zhang *et al.*, Structural basis of STING binding with and phosphorylation by TBK1. *Nature* **567**, 394–398 (2019).
29. X. M. Wang *et al.*, Caveolin-1: A critical regulator of lung fibrosis in idiopathic pulmonary fibrosis. *J. Exp. Med.* **203**, 2895–2906 (2006).
30. C. A. Copeland *et al.*, A disease-associated frameshift mutation in caveolin-1 disrupts caveolae formation and function through introduction of a de novo ER retention signal. *Mol. Biol. Cell* **28**, 3095–3111 (2017).
31. A. Tabarroki *et al.*, Ruxolitinib leads to improvement of pulmonary hypertension in patients with myelofibrosis. *Leukemia* **28**, 1486–1493 (2014).
32. A. T. Low, L. Howard, C. Harrison, R. M. Tulloh, Pulmonary arterial hypertension exacerbated by ruxolitinib. *Haematologica* **100**, e244–e245 (2015).
33. F. Viñals, J. C. Chambard, J. Pouysségur, p70 S6 kinase-mediated protein synthesis is a critical step for vascular endothelial cell proliferation. *J. Biol. Chem.* **274**, 26776–26782 (1999).
34. S. D. S. Oliveira *et al.*, Inflammation-induced caveolin-1 and BMPRII depletion promotes endothelial dysfunction and TGF-β-driven pulmonary vascular remodeling. *Am. J. Physiol. Lung Cell. Mol. Physiol.* **312**, L760–L771 (2017).

35. Y. Y. Zhao *et al*., Persistent eNOS activation secondary to caveolin-1 deficiency induces pulmonary hypertension in mice and humans through PKG nitration. *J. Clin. Invest.* **119**, 2009–2018 (2009).
36. S. D. S. Oliveira, R. D. Minshall, Caveolin and endothelial NO signaling. *Curr. Top. Membr.* **82**, 257–279 (2018).
37. C. A. Chen, L. J. Druhan, S. Varadharaj, Y. R. Chen, J. L. Zweier, Phosphorylation of endothelial nitric-oxide synthase regulates superoxide generation from the enzyme. *J. Biol. Chem.* **283**, 27038–27047 (2008).
38. Z. Chen *et al*., Reciprocal regulation of eNOS and caveolin-1 functions in endothelial cells. *Mol. Biol. Cell* **29**, 1190–1202 (2018).
39. I. Chrobak, S. Lenna, L. Stawski, M. Trojanowska, Interferon-γ promotes vascular remodeling in human microvascular endothelial cells by upregulating endothelin (ET)-1 and transforming growth factor (TGF) β2. *J. Cell. Physiol.* **228**, 1774–1783 (2013).
40. M. Nakano *et al*., Type I interferon induces CX3CL1 (fractalkine) and CCL5 (RANTES) production in human pulmonary vascular endothelial cells. *Clin. Exp. Immunol.* **170**, 94–100 (2012).
41. P. M. George *et al*., Evidence for the involvement of type I interferon in pulmonary arterial hypertension. *Circ. Res.* **114**, 677–688 (2014).
42. K. Fang *et al*., Overexpression of caveolin-1 inhibits endothelial cell proliferation by arresting the cell cycle at G0/G1 phase. *Cell Cycle* **6**, 199–204 (2007).
43. F. Galbiati *et al*., Caveolin-1 expression negatively regulates cell cycle progression by inducing G(0)/G(1) arrest via a p53/p21(WAF1/Cip1)-dependent mechanism. *Mol. Biol. Cell* **12**, 2229–2244 (2001).
44. G. Marsboom *et al*., Aberrant caveolin-1-mediated Smad signaling and proliferation identified by analysis of adenine 474 deletion mutation (c.474delA) in patient fibroblasts: A new perspective on the mechanism of pulmonary hypertension. *Mol. Biol. Cell* **28**, 1177–1185 (2017).
45. A. Navarro, B. Anand-Apte, M. O. Parat, A role for caveolae in cell migration. *FASEB J.* **18**, 1801–1811 (2004).
46. R. Mathew, Pathogenesis of pulmonary hypertension: A case for caveolin-1 and cell membrane integrity. *Am. J. Physiol. Heart Circ. Physiol.* **306**, H15–H25 (2014).
47. A. Beardsley *et al*., Loss of caveolin-1 polarity impedes endothelial cell polarization and directional movement. *J. Biol. Chem.* **280**, 3541–3547 (2005).
48. C. Fernández-Hernando, J. Yu, A. Dávalos, J. Prendergast, W. C. Sessa, Endothelial-specific overexpression of caveolin-1 accelerates atherosclerosis in apolipoprotein E-deficient mice. *Am. J. Pathol.* **177**, 998–1003 (2010).
49. L. Madaro *et al*., Knock down of caveolin-1 affects morphological and functional hallmarks of human endothelial cells. *J. Cell. Biochem.* **114**, 1843–1851 (2013).
50. H. Xu *et al*., Inhibitory effect of caveolin-1 in vascular endothelial cells, pericytes and smooth muscle cells. *Oncotarget* **8**, 76165–76173 (2017).
51. L. G. Rodriguez, X. Wu, J. L. Guan, Wound-healing assay. *Methods Mol. Biol.* **294**, 23–29 (2005).
52. H. Wang, A. X. Wang, E. J. Barrett, Insulin-induced endothelial cell cortical actin filament remodeling: A requirement for trans-endothelial insulin transport. *Mol. Endocrinol.* **26**, 1327–1338 (2012).
53. M. W. Geraci *et al*., Gene expression patterns in the lungs of patients with primary pulmonary hypertension: A gene microarray analysis. *Circ. Res.* **88**, 555–562 (2001).
54. R. M. Tuder, B. Groves, D. B. Badesch, N. F. Voelkel, Exuberant endothelial cell growth and elements of inflammation are present in plexiform lesions of pulmonary hypertension. *Am. J. Pathol.* **144**, 275–285 (1994).
55. E. Stacher *et al*., Modern age pathology of pulmonary arterial hypertension. *Am. J. Respir. Crit. Care Med.* **186**, 261–272 (2012).
56. M. Humbert *et al*., Pathology and pathobiology of pulmonary hypertension: State of the art and research perspectives. *Eur. Respir. J.* **53**, 1801887 (2019).
57. D. D. Taub *et al*., Recombinant human interferon-inducible protein 10 is a chemoattractant for human monocytes and T lymphocytes and promotes T cell adhesion to endothelial cells. *J. Exp. Med.* **177**, 1809–1814 (1993).
58. G. A. Heresi, M. Aytekin, J. Newman, R. A. Dweik, CXC-chemokine ligand 10 in idiopathic pulmonary arterial hypertension: Marker of improved survival. *Lung* **188**, 191–197 (2010).
59. O. Sanchez *et al*., Role of endothelium-derived CC chemokine ligand 2 in idiopathic pulmonary arterial hypertension. *Am. J. Respir. Crit. Care Med.* **176**, 1041–1047 (2007).
60. P. Dorfmüller *et al*., Chemokine RANTES in severe pulmonary arterial hypertension. *Am. J. Respir. Crit. Care Med.* **165**, 534–539 (2002).
61. J. M. Elinoff *et al*., Meta-analysis of blood genome-wide expression profiling studies in pulmonary arterial hypertension. *Am. J. Physiol. Lung Cell. Mol. Physiol.* **318**, L98–L111 (2019).
62. T. Saito *et al*., Upregulation of human endogenous retrovirus-K is linked to immunity and inflammation in pulmonary arterial hypertension. *Circulation* **136**, 1920–1935 (2017).
63. Y. Y. Bustamante Rivera, C. Brütting, C. Schmidt, I. Volkmer, M. S. Staege, Endogenous retrovirus 3—History, physiology, and pathology. *Front. Microbiol.* **8**, 2691 (2018).
64. M. Mangeney *et al*., Placental syncytins: Genetic disjunction between the fusogenic and immunosuppressive activity of retroviral envelope proteins. *Proc. Natl. Acad. Sci. U.S.A.* **104**, 20534–20539 (2007).
65. N. Sasaki *et al*., Human endogenous retrovirus-R Env glycoprotein as possible autoantigen in autoimmune disease. *AIDS Res. Hum. Retroviruses* **25**, 889–896 (2009).
66. K. S. Awad *et al*., Raf/ERK drives the proliferative and invasive phenotype of BMPR2-silenced pulmonary artery endothelial cells. *Am. J. Physiol. Lung Cell. Mol. Physiol.* **310**, L187–L201 (2016).
67. H. Cheon, G. R. Stark, Unphosphorylated STAT1 prolongs the expression of interferon-induced immune regulatory genes. *Proc. Natl. Acad. Sci. U.S.A.* **106**, 9373–9378 (2009).
68. M. Chatterjee-Kishore, K. L. Wright, J. P. Ting, G. R. Stark, How Stat1 mediates constitutive gene expression: A complex of unphosphorylated Stat1 and IRF1 supports transcription of the LMP2 gene. *EMBO J.* **19**, 4111–4122 (2000).
69. S. W. Ryter, A. M. Choi, H. P. Kim, Profibrogenic phenotype in caveolin-1 deficiency via differential regulation of STAT-1/3 proteins. *Biochem. Cell Biol.* **92**, 370–378 (2014).
70. F. A. Masri *et al*., Hyperproliferative apoptosis-resistant endothelial cells in idiopathic pulmonary arterial hypertension. *Am. J. Physiol. Lung Cell. Mol. Physiol.* **293**, L548–L554 (2007).
71. J. E. Durbin, R. Hackenmiller, M. C. Simon, D. E. Levy, Targeted disruption of the mouse Stat1 gene results in compromised innate immunity to viral disease. *Cell* **84**, 443–450 (1996).
72. S. R. Chan *et al*., STAT1-deficient mice spontaneously develop estrogen receptor α-positive luminal mammary carcinomas. *Breast Cancer Res.* **14**, R16 (2012).
73. C. Schneckenleithner *et al*., Putting the brakes on mammary tumorigenesis: Loss of STAT1 predisposes to intraepithelial neoplasias. *Oncotarget* **2**, 1043–1054 (2011).
74. L. M. Hix *et al*., Tumor STAT1 transcription factor activity enhances breast tumor growth and immune suppression mediated by myeloid-derived suppressor cells. *J. Biol. Chem.* **288**, 11676–11688 (2013).
75. N. Khodarev *et al*., Cooperativity of the MUC1 oncoprotein and STAT1 pathway in poor prognosis human breast cancer. *Oncogene* **29**, 920–929 (2010).
76. E. F. Morand *et al*.; TULIP-2 Trial Investigators, Trial of anifrolumab in active systemic lupus erythematosus. *N. Engl. J. Med.* **382**, 211–221 (2020).
77. H. Nguyen, C. V. Ramana, J. Bayes, G. R. Stark, Roles of phosphatidylinositol 3-kinase in interferon-gamma-dependent phosphorylation of STAT1 on serine 727 and activation of gene expression. *J. Biol. Chem.* **276**, 33361–33368 (2001).
78. R. Haq *et al*., Regulation of erythropoietin-induced STAT serine phosphorylation by distinct mitogen-activated protein kinases. *J. Biol. Chem.* **277**, 17359–17366 (2002).
79. D. A. Goncharov *et al*., Mammalian target of rapamycin complex 2 (mTORC2) coordinates pulmonary artery smooth muscle cell metabolism, proliferation, and survival in pulmonary arterial hypertension. *Circulation* **129**, 864–874 (2014).
80. National Research Council, *Guide for the Care and Use of Laboratory Animals* (National Academies Press, Washington, DC, ed. 8, 2011).